Contribution from the Chemistry Department,
University of California, Davis, California 95616

Reactions of Low-Coordinate Transition-Metal Amides with Secondary Phosphanes and Arsanes: Synthesis, Structural, and Spectroscopic Studies of $[M\{N(SiMe_3)_2\}(\mu\text{-}PMes_2)]_2$ (M = Mn, Fe), $[Mn\{N(SiMe_3)_2\}(\mu\text{-}AsMes_2)]_2$, and $Mes_2AsAsMes_2$

Hong Chen, Marilyn M. Olmstead, Doris C. Pestana, and Philip P. Power*

Received September 18, 1990

The reactions of the transition-metal amides $M[N(SiMe_3)_2]_2$ (M = Mn, Fe) with dimesitylphosphane or dimesitylarsane, $HPMes_2$ or $HAsMes_2$, (Mes = 2,4,6-$Me_3C_6H_2$) have been investigated. For the reactions involving 1 or 2 equiv of $HPMes_2$, the major products are the dimers $[M\{N(SiMe_3)_2\}(\mu\text{-}PMes_2)]_2$ (M = Mn (**1**), Fe (**2**)). These complexes feature three-coordinate metals with phosphide bridges and terminal amide groups. A similar product, $[Mn\{N(SiMe_3)_2\}(\mu\text{-}AsMes_2)]_2$ (**3**), is obtained from the reaction between $Mn[N(SiMe_3)_2]_2$ and either 1 or 2 equiv of $HAsMes_2$. When $Fe[N(SiMe_3)_2]_2$ is treated with 1 or 2 equiv of $HAsMes_2$, however, tetramesityldiarsane, $Mes_2AsAsMes_2$, (**4**), is formed. The X-ray crystal structures of **1**–**4** were determined by X-ray crystallography. The metal complexes were further characterized by electronic absorption spectroscopy and magnetic data. Variable-temperature ^1H NMR spectroscopy of **1** and **4** is also reported. Crystal data with Mo Kα (λ = 0.71069 Å) radiation at 130 K: **1**, $[Mn\{N(SiMe_3)_2\}(\mu\text{-}PMes_2)]_2$, $C_{48}H_{80}Mn_2N_2P_2Si_4$, a = 20.480 (14) Å, b = 11.808 (14) Å, c = 23.331 (9) Å, β = 106.39 (4)°, Z = 4, monoclinic, space group $P2_1/c$, R = 0.053; **2**, $[Fe\{N(SiMe_3)_2\}(\mu\text{-}PMes_2)]_2$, $C_{48}H_{80}Fe_2N_2P_2Si_4$, a = 12.459 (3) Å, b = 19.438 (6) Å, c = 24.794 (6) Å, α = 67.43 (2)°, β = 84.78 (2)°, γ = 80.68 (2)°, Z = 4, triclinic, space group $P\bar{1}$, R = 0.099; **3**, $[Mn\{N(SiMe_3)_2\}(\mu\text{-}AsMes_2)]_2$, $C_{48}H_{80}As_2Mn_2N_2Si_4$, a = 20.549 (8) Å, b = 11.801 (6) Å, c = 23.467 (10) Å, β = 106.01 (3)°, Z = 4, monoclinic, space group $P2_1/c$, R = 0.070; **4**, $Mes_2AsAsMes_2$, $C_{36}H_{44}As_2$, a = 8.857 (2) Å, c = 39.715 (14) Å, Z = 4, tetragonal, space group $P4_32_12$, R = 0.072.

Introduction

The most extensively studied reactions of dialkylamido and bis(trimethylsilyl)amido derivatives of transition metals are, perhaps, those with protic species. Numerous papers have described these reactions with alcohols,[1-6] with thiols,[7,8] and with hydrocarbons that have acidic C–H bonds such as cyclopentadiene[9-11] and indene.[10] Much less is known about the reactivity of metal amides toward primary or secondary phosphanes or arsanes. These reactions are of interest in that they are a potential route to transition-metal phosphides. Such a route should possess the significant advantage of avoiding the use of reducing alkali-metal phosphide precursors. In addition, the question of the inclusion of alkali-metal ions or salts as part of the metal phosphide product does not arise with the use of an easily purified amide precursor. Well-characterized transition-metal phosphides such as $Mo(PCy_2)_4$[12] and $Mo[P(t\text{-}Bu)_2][\mu\text{-}P(t\text{-}Bu)_2]_2$[13] and transition-metal complexes that involve both phosphide and amide ligands, for example $M_2[P(t\text{-}Bu)_2]_2[NMe_2]_4$ (M = Mo or W),[14] have been described, but these were synthesized by the reaction of $LiPR_2$ with the metal halide or metal amide halide. The most relevant prior research to the work in this paper has involved the treatment of the species $[Mn\{CH_2(t\text{-}Bu)\}_2]_n$ with $HP(t\text{-}Bu)_2$ to give the compound $[MnCH_2(t\text{-}Bu)\{\mu\text{-}P(t\text{-}Bu)_2\}]_2$,[15] which has a dimeric phosphido-bridged structure. In addition, a recent publication has described the syntheses and structures of homoleptic silylphosphido complexes $[M\{P(SiMe_3)_2\}\{\mu\text{-}P(SiMe_3)_2\}]_2$ (M = Zn or Cd)[16] from the amide precursor and the phosphane $HP(SiMe_3)_2$. These later results, however, are at present restricted to species with closed-shell (d^{10}) configurations or, in the case of the open-shell compound, to homoleptic metal alkyl precursors, which are often difficult to make or are unknown for many later transition metals. Some previous studies in this laboratory have focused on the structural characterization of low-coordinate, open-shell (d^0–d^9) transition-metal amide complexes and the reactivities of these complexes with various bulky lithium reagents and sterically demanding alcohols and silanols.[2-4,17] This work is now extended to reactivity studies toward the bulky diarylphosphane and diarylarsane molecules, $HPMes_2$ and $HAsMes_2$.

Experimental Section

General Procedures. All work was performed under anaerobic and anhydrous conditions by using Schlenk techniques under N_2 or a Vacuum Atmospheres HE 43-2 drybox. Solvents were freshly distilled under N_2 from Na/K or sodium/potassium benzophenone ketyl and degassed twice immediately before use. ^1H NMR spectra were obtained on a General Electric QE-300 spectrometer. Electronic absorption spectra were obtained on a Hewlett Packard 8450A UV/vis spectrometer. Magnetic moment measurements were performed via the Evans method.[18] All compounds gave satisfactory C, H, and N analyses.

Starting Materials. $HPMes_2$ was synthesized via a modified literature procedure.[19,20] Two equivalents of MesMgBr in THF (ca. 1 M concentration) were added to PCl_3 in THF/Et_2O, the resulting Mes_2PCl was purified by crystallization from hexane. This was followed by the reduction of Mes_2PCl with $LiAlH_4$ in Et_2O and purification of the final product, $HPMes_2$, by recrystallization from hexane. $HAsMes_2$ was prepared by previously described procedures.[21] A 1.6 M *n*-BuLi in hexane solution (Aldrich), $MnBr_2$ (Aldrich), and $FeBr_2$ (Cerac) were used as received. $Mn[N(SiMe_3)_2]_2$ was synthesized via a slight modification of a published procedure.[22] $Fe[N(SiMe_3)_2]_2$ was also isolated as described in the literature.[23]

(1) Lappert, M. F.; Power, P. P.; Sanger, A. R.; Srivastava, R. C. *Metal and Metalloid Amides*; Ellis Horwood: Chichester, England, 1980.
(2) Olmstead, M. M.; Sigel, G. A.; Hope, H.; Xu, X.; Power, P. P. *J. Am. Chem. Soc.* **1985**, *107*, 8087.
(3) Murray, B. D.; Hope, H.; Power, P. P. *J. Am. Chem. Soc.* **1985**, *107*, 169.
(4) Sigel, G. A.; Bartlett, R. A.; Decker, D.; Olmstead, M. M.; Power, P. P. *Inorg. Chem.* **1987**, *26*, 1773.
(5) Abel, E. W.; Armitage, D. A.; Brady, D. B. *J. Organometallic Chem.* **1966**, *5*, 130.
(6) Lappert, M. F.; Sanger, A. R. *J. Chem. Soc. A* **1971**, 1314.
(7) Shoner, S. C.; Power, P. P. Unpublished results.
(8) Bradley, D. C.; Chisholm, M. H.; Extine, M. W.; Stager, M. E. *Inorg. Chem.* **1977**, *16*, 1794.
(9) Chandra, G.; Lappert, M. F. *J. Chem. Soc. A* **1968**, 1940.
(10) Jenkins, A. D.; Lappert, M. F.; Srivastava, R. C. *J. Organomet. Chem.* **1970**, *23*, 165.
(11) Jamerson, J. D.; Takats, J. *J. Organomet. Chem.* **1974**, *78*, C23.
(12) Baker, R. T.; Krusic, P. J.; Tulip, T. H.; Calabrese, J. C.; Wreford, S. S. *J. Am. Chem. Soc.* **1983**, *105*, 6763.
(13) Jones, R. A.; Lasch, J. G.; Norman, N. C.; Whittlesey, B. R.; Wright, T. C. *J. Am. Chem. Soc.* **1983**, *105*, 6184.
(14) Buhro, W. E.; Chisholm, M. H.; Folting, K.; Huffman, J. C. *J. Am. Chem. Soc.* **1987**, *109*, 905.
(15) Jones, R. A.; Koschmieder, S. U.; Nunn, C. M. *Inorg. Chem.* **1988**, *27*, 4526.
(16) Goel, S. C.; Chiang, M. Y.; Buhro, W. E. *J. Am. Chem. Soc.* **1990**, *112*, 5636.
(17) Murray, B. D.; Power, P. P. *Inorg. Chem.* **1984**, *23*, 4584. Bradley, D. C.; Hursthouse, M. B.; Malik, K. M. A.; Moseler, R. *Transition Met. Chem. (Weinheim, Ger.)* **1978**, *3*, 253.
(18) Evans, D. F. *J. Chem. Soc.* **1959**, 2005.
(19) Fritzsche, H.; Hasserodt, U.; Korte, F. *Chem. Ber.* **1965**, *98*, 1681.
(20) Bartlett, R. A.; Olmstead, M. M.; Power, P. P.; Sigel, G. A. *Inorg. Chem.* **1987**, *26*, 1941.
(21) Pitt, C. G.; Purdy, A. P.; Higa, K. T.; Wells, R. L. *Organometallics*, **1986**, *5*, 1266.
(22) Bürger, H.; Wannagat, U. *Monatsh. Chem.* **1964**, *95*, 1099. The route employed in this laboratory involves $MnBr_2$, $LiN(SiMe_3)_2$, and Et_2O instead of MnI_2, $NaN(SiMe_3)_2$, and THF.

0020-1669/91/1330-1783$02.50/0

Table I. Crystallographic Data for Compounds **1–4**

	1	2	3	4
compound	$[Mn\{N(SiMe_3)_2\}(\mu\text{-}PMes_2)]_2$	$[Fe\{N(SiMe_3)_2\}(\mu\text{-}PMes_2)]_2$	$[Mn\{N(SiMe_3)_2\}(\mu\text{-}AsMes_2)]_2$	$Mes_2AsAsMes_2$
formula	$C_{48}H_{80}Mn_2N_2P_2Si_4$	$C_{48}H_{80}Fe_2N_2P_2Si_4$	$C_{48}H_{80}As_2Mn_2N_2Si_4$	$C_{36}H_{44}As_2$
fw	969.34	971.16	1057.2	626.6
color and habit	green-gold dichroic parallelepipeds	black-red rhombs	green-gold dichroic parallelepipeds	colorless plates
space group	$P2_1/c$	$P\bar{1}$	$P2_1/c$	$P4_32_12$
a, Å	20.480 (14)	12.459 (7)	20.549 (8)	8.857 (2)
b, Å	11.808 (5)	19.438 (6)	11.801 (6)	
c, Å	23.331 (9)	24.794 (6)	23.467 (10)	39.715 (14)
α, deg		67.43 (2)		
β, deg	106.39 (4)	84.78 (2)	106.01 (3)	
γ, deg		80.68 (2)		
V, Å^3	5413 (5)	5469 (3)	5470 (4)	3115.8 (15)
Z	4	4	4	4
T, K	130	130	130	130
radiation (λ, Å)	0.71069	0.71069	0.71069	0.71069
μ(Mo Kα), cm^{-1}	6.2	7.0	17.6	21.6
range transm factors	0.85–0.86	0.86–0.93	0.77–0.83	0.47–0.79
$R(F)$, $R_w(F)$	0.053, 0.060	0.099, 0.092	0.070, 0.62	0.072, 0.072

Table II. Important Bond Distances (Å) and Angles (deg) and Other Structural Parameters for Compounds **1–3**, **5** ($Mn[N(SiMe_3)_2]_2$[17]), **6** ($Fe[N(SiMe_3)_2]_2$[29]), and **7** ($[Mn\{CH_2(t\text{-}Bu)\}\{P(t\text{-}Bu)_2\}]_2$[15])

	1	2	3	5	6	7
M–E[a](bridging)	2.524 (3)	2.390 (5)	2.610 (2)	2.172 (3)	2.085 (2)	2.501 (4)
M–N(terminal)	1.973 (5)	1.914 (14)	1.960 (8)	1.998 (3)	1.925 (3)	2.280 (2)[b]
M···M	3.364 (2)	2.894 (2)	3.676 (2)	2.881 (1)	2.663 (1)	3.293 (2)
M–E–M	83.6 (1)	74.6 (2)	89.6 (1)	80.6 (1)	79.4 (1)	82.4 (2)
E–M–E	94.5 (1)	103.4 (2)	88.7 (1)	99.2 (1)	100.7 (1)	97.6 (2)
Si–N–Si	124.1 (3)	122.0 (9)	125.6 (5)	119.1 (3)	119.6 (2)	
angle between MEE planes	158.1	155.0	160.2			

[a] E = N, P, As. [b] Mn–C bond length.

Syntheses of Compounds 1–4. $[M\{N(SiMe_3)_2\}(\mu\text{-}PMes_2)]_2$ (M = Mn (1), Fe (2)). $M[N(SiMe_3)_2]_2$ (2 mmol, 0.75 g; M = Mn[22] or Fe[23]) and $HPMes_2$ (2 mmol, 0.54 g) were heated together at 100 °C in a Schlenk tube. The mixture became yellowish green, for M = Mn, or dark red, for M = Fe, upon heating for 5 min. The volatile byproduct $HN(SiMe_3)_2$ was removed under reduced pressure, which produced concomitant solidification of the residue. The solid was extracted with hexane (20 mL), and the solution was filtered and its volume then reduced to ca. 10 mL under reduced pressure. Cooling overnight in a −20 °C freezer gave the product $[Mn\{N(SiMe_3)_2\}(\mu\text{-}PMes_2)]_2$ (**1**) as yellowish green crystals (yield 0.53 g, 55%; mp = 222–225 °C) and $[Fe\{N(SiMe_3)_2\}(\mu\text{-}PMes_2)]_2$ (**2**) as dark red crystals [yield 0.29 g, 30%; mp = 86–89 °C]. Anal. Calcd for **1**, $C_{48}H_{80}N_2P_2Si_4Mn_2$: C, 59.49; H, 8.32; N, 2.9. Found: C, 59.8; H, 8.5; N, 2.8. Calcd for **2**, $C_{48}H_{80}N_2P_2Si_4Fe_2$: C, 59.36; H, 8.3; N, 2.88. Found C, 59.8; H, 8.43; N, 2.81.

$[Mn\{N(SiMe_3)_2\}(\mu\text{-}AsMes_2)]_2$ (3). $Mn[N(SiMe_3)_2]_2$ (2 mmol, 0.75 g) and $HAsMes_2$ (2 mmol, 0.63 g) were mixed and heated to ca. 100 °C for 5 min. The volatile material was then removed under reduced pressure, to give the crude product as a yellowish green solid. Purification was performed by dissolving the solid in hexane (30 mL). Subsequent filtration and evaporation under reduced pressure to induce crystallization (~15 mL total volume) afforded **3** as yellowish green crystals upon slow cooling to −20 °C for 12 h (yield 0.54 g, 51%; mp = 120 °C dec). Anal. Calcd for $C_{48}H_{80}N_2As_2Si_4Mn_2$: C, 54.53; H, 7.63; N, 2.65. Found: C, 54.7; H, 7.8; N, 2.62.

$Mes_2AsAsMes_2$ (4). $Fe[N(SiMe_3)_2]_2$[23] (2 mmol, 0.75 g) and $HAsMes_2$ (2 mmol, 0.63 g) mixture was treated in a manner similar to that described for **3**. Upon workup, however, tetramesityldiarsine, $Mes_2AsAsMes_2$ (**4**), was isolated as large brown crystals, instead of the expected amidoiron arsinide. Subsequent recrystallization from hexane gave the pure product as colorless crystals (yield 0.29 g, 46%; mp = 270–271 °C).

Reactions of $Co[N(SiMe_3)_2]_2$[24] with $HPMes_2$ or $HAsMes_2$. $Co[N(SiMe_3)_2]_2$ (2 mmol, 0.75 g) and $HPMes_2$ (4 mmol, 1.08 g) or $HAsMes_2$ (4 mmol, 1.26 g) mixture was treated in a manner similar to that for **3**. Upon workup, however, no crystalline product was obtained from the resultant blue solution.

X-ray Data Collection, Solution, and Refinement of the Structures. The X-ray data for compounds **1** and **4** were collected by using a Syntex $P2_1$ diffractometer equipped with a locally modified Syntex LT-1 device.

Table III. Magnetic Moments (μ_B) and Electronic Absorption Spectral Data for Compounds **1–3** (cm^{-1}) with ϵ Values in Parenthese

	1	2	3
magnetic moments	5.91	4.94	6.65
electronic abs data	20450 (138)	20000 (1630)	26250 (623)
	16400 (61)	12500 (171)	25200 (422)

Data collections for compounds **2** and **3** were carried out on a Siemens R3m/v diffractometer equipped with a locally modified Enraf-Nonius LT apparatus. All calculations were carried out on a Micro VAX 3200 using the SHELTXL PLUS program system. The atom form factors, including anomalous scattering were from ref 25. Crystals of **1–4** were transferred from the Schlenk tubes under N_2 to Petri dishes and immediately covered with a layer of hydrocarbon oil.[26] A single crystal was selected, mounted on a glass fiber and immediately placed in a low-temperature N_2 stream. Some details of the data collection and refinement are given in Table I. Further details are provided in the supplementary material. The important bond distances, angles, and other structural parameters for compounds **1–4** are listed in Table II. All structures were solved by direct methods. An absorption correction was applied in each case.[27] Hydrogen atoms were included in the refinement at calculated positions by using a riding model, with C–H of 0.96 Å and $U_H = 1.2U_C$ for compound **1**, $U_H = 0.05$ for compound **2**, $U_H = 0.03$ for **3**, and $U_H = 0.04$ (methyl groups) and $U_H = 0.05$ (phenyl hydrogens) in compound **4**. All non-hydrogen atoms were refined anisotropically except in the case of the structures of **2**, where only Fe, P, N, Si, atoms and C atoms attached to Si were made anisotropic, and in the case of **4**, where only the arsenic was refined anisotropically. Below average crystal quality resulted in a higher than usual R factor for **2**. The largest features on the final difference maps were 0.58, 0.91, 0.80 and 0.90 e/Å^3 for **1–4**, respectively. The mean shift/esd values are 0.005, 0.002, 0.001, and 0.008.

(23) Andersen, R. A.; Faegri, K., Jr.; Green, J. C.; Haaland, A.; Lappert, M. F.; Leung, W.-P.; Rypdal, K. *Inorg. Chem.* **1988**, 27, 1782.
(24) Bürger, H.; Wannagat, U. *Monatsh. Chem.* **1963**, *94*, 1007.
(25) *International Tables for X-ray Crystallography*; Kynoch Press: Birmingham, England, 1974; Vol. IV.
(26) This method is described in: Hope, H In *Experimental Organometallic Chemistry: A Practicum in Synthesis and Characterization*; Wayda, A. L., Darensbourg, M. Y., Eds.; ACS Symposium Series 357; American Chemical Society: Washington, D.C., 1987; Chapter 10.
(27) The absorption correction was made using program XABS by H. Hope and B. Moezzi. The program obtains an absorption tensor from $F_o - F_c$ differences. B. Moezzi, Ph.D. Dissertation, University of California, Davis, 1987.

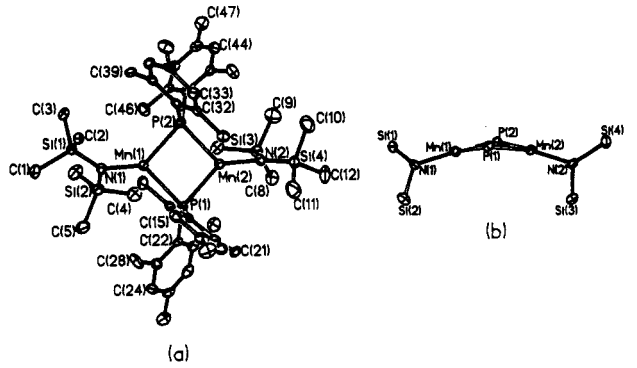

Figure 1. (a) Computer-generated plot of **1**. Hydrogen atoms are omitted for clarity. (b) View of the core atoms of **1** along the P(1)···P(2) direction.

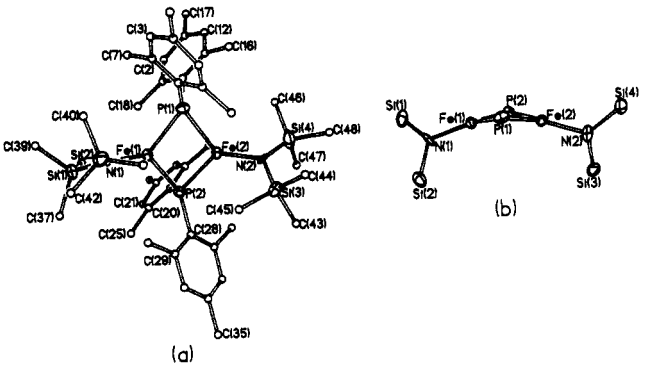

Figure 2. (a) Computer-generated plot of **2**. Hydrogen atoms are omitted for clarity. (b) View of the core atoms of **2** along the P(1)···P(2) direction.

Electronic Absorption and Magnetic Measurements. The electronic absorption spectra of compounds **1–3** were recorded in hexane. The data are summarized in Table III. The magnetic moments of compounds **1–3** are also provided in Table III. These were measured at 297.3 K in C_6D_6/C_6H_6 solution via the Evans method.[18] The shifts were measured relative to the residual C_6H_6, which afforded frequency differences in the range of 200–620 Hz at 300 MHz. Variable-temperature ^1H NMR data from **1** and **4** were recorded on solutions in toluene-d_8.

Results and Discussion

Structural Descriptions. $[Mn\{N(SiMe_3)_2\}(\mu\text{-}PMes_2)]_2$ (1). The molecular structure of **1** is illustrated in Figure 1a. Its structure consists of discrete molecules of dimeric $[Mn\{N(SiMe_3)_2\}(\mu\text{-}PMes_2)]_2$ units that are well separated from each other and have no imposed crystallographic symmetry. The metals possess approximate trigonal-planar coordination with the $\Sigma°$ at Mn(1) and Mn(2) = 359.5 and 347.6°. The angles at the metals are very irregular and vary from 94.2 (2) to 136.6 (2)°. The average Mn–P and Mn–N distances are 2.524 (3) and 1.973 (5) Å, respectively. Within the Mn_2P_2 core, the average P–Mn–P and Mn–P–Mn angles are 94.5 and 83.6° and the separation of the two Mn atoms is 3.364 (2) Å. The nitrogen centers have trigonal-planar coordination, but the central Mn_2P_2 ring is folded and the dihedral angle between the two MnPP planes is 158.1° (see Figure 1b). The angles between the N(1)–Mn(1) and N(2)–Mn(2) bonds and the corresponding MnPP planes are 5.4 and 5.9°. The torsion angles P(2)Mn(1)P(1)Mn(2) and P(2)Mn(2)P(1)Mn(1) are 14.7 and 14.8°, respectively.

$[Fe\{N(SiMe_3)_2\}(\mu\text{-}PMes_2)]_2$ (2). The structure of **2** is illustrated in Figure 2a and consists of well-separated molecules of $[Fe\{N(SiMe_3)_2\}(\mu\text{-}PMes_2)]_2$ dimers that have no crystallographic symmetry. The asymmetric unit contains two molecules that differ only slightly from each other. Apart from small differences in the bond lengths and angles, the structure is remarkably similar to **1**. The corresponding bond lengths and angles for both molecules are given in Table II. A distorted-trigonal-planar coordination is observed for the iron centers. The average Fe–P and Fe–N distances are 2.390 (6) and 1.914 (14) Å, respectively, and the separation of the two Fe atoms averages 2.921 (2) Å. Each nitrogen center possesses trigonal-planar coordination. As in **1**, the metal phosphorus core is folded and the average angle between FePP planes is 155° (see Figure 2b). The angles between Fe(1)–N(1) and Fe(2)–N(2) bonds and the corresponding FePP planes are 8.3 and 6.4°. The average torsional angles for the arrays P(2)Fe(1)P(1)Fe(2) and P(2)Fe(2)P(1)Fe(1) are 15.9 and 15.8°, respectively.

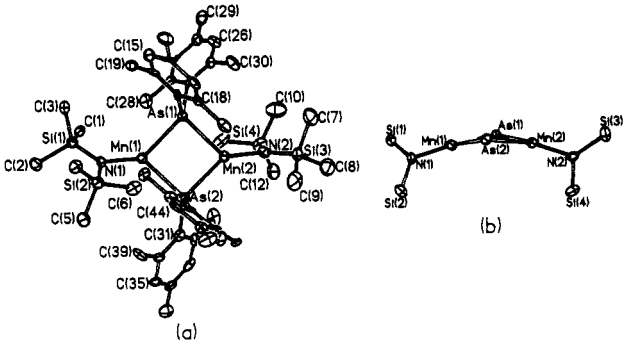

Figure 3. (a) Computer-generated plot of **3**. Hydrogen atoms are omitted for clarity. (b) View of the core atoms of **3** along the As(1)···As(2) direction.

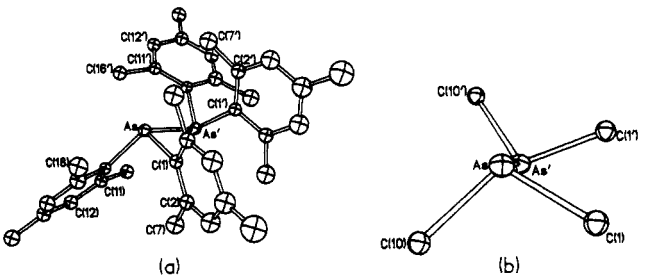

Figure 4. (a) Computer-generated plot of **4**. Hydrogen atoms are omitted for clarity. (b) View of the core atoms of **4** along the As–As′ axis. Important bond lengths (Å) and angles (deg) are listed as follows: As–As′ = 2.472 (3), As–C(1) = 1.964 (12), As–C(10) = 1.995 (11); C(1)–As–C(10) = 102.6 (5), C(1)–As–As′ = 94.1 (4), C(10)–As–As′ = 109.6 (3).

$[Mn\{N(SiMe_3)_2\}(\mu\text{-}AsMes_2)]_2$ (3). The crystals of **3** are isomorphous with those of **1**. Not surprisingly, its structure, which is illustrated in Figure 3a, also bears a close resemblance to that of **1**, with well-separated molecular units of $[Mn\{N(SiMe_3)_2\}(\mu\text{-}AsMes_2)]_2$ that have no imposed symmetry restrictions. The average Mn–As and Mn–N distances are 2.610 (2) and 1.960 (8) Å, respectively and the distance between two Mn atoms is 3.676 (2) Å. In addition, the nitrogen centers possess trigonal-planar coordination. In the Mn_2As core, the average As–Mn–As angle is 88.7° and the average Mn–As–Mn angle is 89.6°. The core Mn_2As_2 ring is also folded (see Figure 3b, and the angle between MnAsAs planes is 160.2°. The angles between Mn(1)–N(1) and Mn(2)–N(2) bonds and the corresponding MnAsAs planes are 6.7 and 10.7°. The torsion angles As(2)Mn(1)As(1)Mn(2) and As(2)Mn(2)As(1)Mn(1) are 14.0 and 14.0°, respectively.

$Mes_2AsAsMes_2$ (4). The structure of **4** is illustrated in Figure 4a. It consists of well-separated molecules of $Mes_2AsAsMes_2$ that possess a 2-fold rotation axis perpendicular to and through the center of the As–As′ bond. The As–As′ bond length is 2.472 (3) Å, and the arsenic centers have pyramidal coordination with $\Sigma°$ (at As) = 306.3°. The length of the As–C(1) and As–C(10) bonds are 1.964 (12) and 1.995 (11) Å, respectively. The angles at arsenic display considerable asymmetry. The C(10)–As–As′ angle, 109.6 (3)°, is over 15° wider than C(1)–As–As′, 94.1 (4)°. A view of the molecule along the As–As′ axis is presented in Figure 4b, which shows that the torsion angles C(1)AsAs′C(1)′ and C(10)AsAsC(10)′ are 51.2 and 99.0° respectively.

Discussion

The syntheses of compounds **1–4** are greatly facilitated by the ready availability of the bis[bis(trimethylsilyl)amido]manga-

nese(II) and -iron(II) precursors.[22,23] When either $M[N(SiMe_3)_2]_2$ complex (M = Mn, Fe) is treated with 1 or 2 equiv of $HPMes_2$, only one of the bis(trimethylsilyl)amido ligands is replaced by a dimesitylphosphide group. The latter group is invariably found in the bridging position in both complexes. A similar result was obtained from the reaction between $Mn[N(SiMe_3)_2]_2$ and $HAsMes_2$. The reaction between $Fe[N(SiMe_3)_2]_2$ and $HAsMes_2$, however, resulted in the formation of tetramesityldiarsane. These reactions, which proceeded smoothly and in moderate yield, may be summarized by the following equations:

$$M[N(SiMe_3)_2]_2 + (1 \text{ or } 2)HPMes_2 \rightarrow \tfrac{1}{2}[M\{N(SiMe_3)_2\}(\mu\text{-}PMes_2)]_2 + HN(SiMe_3)_2$$
M = Mn (**1**) or Fe (**2**)

$$Mn[N(SiMe_3)_2]_2 + (1 \text{ or } 2)HAsMes_2 \rightarrow \tfrac{1}{2}[Mn\{N(SiMe_3)_2\}(\mu\text{-}AsMes_2)]_2 + HN(SiMe_3)_2$$
3

$$Fe[N(SiMe_3)_2]_2 + HAsMes_2 \rightarrow Mes_2AsAsMes_2 \text{ (major product)}$$
4

Attempts to replace the second amide group by dimesitylphosphide or arsenic ligands resulted in either intractable products or decomposition. For example, harsher reaction conditions, in which the reaction mixtures were heated to about 200 °C for 15 min and thereafter refluxed in toluene overnight, generally resulted in a change in the color of the mixtures from green to brown. For the reaction between $Mn[N(SiMe_3)_2]_2$ and dimesitylphosphane, however, no pure products have been obtained to date. In the case of the $Mn[N(SiMe_3)_2]_2$ and dimesitylarsane mixture, tetramesityldiarsane was isolated. The reaction between $Fe[N(SiMe_3)_2]_2$ and $HAsMes_2$ also afforded $Mes_2AsAsMes_2$.

The reluctance to substitute the second metal–amide ligand is probably due to steric crowding. In **1–3** the metals remain three-coordinate and are surrounded by three bulky groups. Consistent with the excellent bridging properties of phosphido ligands, there is no evidence for dissociation of the dimers to give less crowded and more reactive two-coordinate monomers. In sharp contrast, the precursors $M[N(SiMe_3)_2]_2$ (M = Mn or Fe) are dimeric in the solid state but dissociate to give more reactive monomers in solution.[28,29] The presence of the diarsane in the reaction mixtures underscores the tendency of the homoleptic transition-metal phosphides and arsinides to decompose to a stable diphosphane or diarsane when heated.[30] The driving force for this decomposition is probably the strength of the P–P bond and the (relative) weakness of the M–P bonds. An extreme example of this decomposition tendency is observed where the resulting P–P or As–As bonds are especially strong. For instance, the species $(PRBMes_2)_2$ (R = 1-adamantyl or Mes), which have very short (~2.11 Å) and strong P–P single bonds, are formed, even below room temperture, when $LiPRBMes_2$ salts are added to $MX_{2 \text{ or } 3}$ (M = Cr, Mn, Fe; X = Cl, Br).[31] This behavior of the metal phosphides is in sharp contrast to their lower homologues, the metal amides, which exhibit much greater thermal stability. In the case of the latter, the relatively strong M–N bonds and weak N–N bonds do not favor the type of decomposition seen with phosphides and arsenides.

Structures. The salient features of the structures of **1–4** have been outlined above. The structure of **4** needs little further comment except to note that it is quite similar to the structure of its phosphorus analogue, tetramesityldiphosphane.[32] It thus has the anti conformation, and it possesses rigorous C_2 symmetry. The As–As distance is 2.472 (3) Å. Few diarsanes have been structurally characterized. Exceptions involve the species $Ph_2AsAsPh_2$,[33] which has an As–As bond length of 2.458 (1) Å with the phenyl groups in a staggered configuration, and the salt $[Li(thf)\{As(t\text{-}Bu)As(t\text{-}Bu)_2\}]_2$,[34] which has an As–As bond length of 2.403 (2) Å. Although the As–As bond distance in **4** is marginally longer than these, it is notable that similar As–As bond lengths of ~2.45–2.47 Å have also been observed in such compounds as cyclopolyarsanes and their transition-metal complexes.[35] It is possible that the marginally longer distances in both the latter species and in **4** are a consequence of the steric congestion. Consistent with this view, a relatively long P–P bond of 2.260 (1) Å was also observed in the crowded diphosphane Mes_2PPMes_2.[32]

The structures of **1–3** may be compared with those of the previously reported dimers $[M\{N(SiMe_3)_2\}_2]_2$ (M = Mn[17] (**5**), Fe (**6**)[29] and with $[Mn\{CH_2(t\text{-}Bu)\}\{\mu\text{-}P(t\text{-}Bu)_2\}]_2$ (**7**) (Table II).[15] Clearly, there is a broad resemblance in that all the compounds are dimeric and feature approximately planar, three-coordinate metal geometries. The structures of **1–3**, like **7**, have an M_2E_2 (E = P or As) instead of an M_2N_2 core structure. As a consequence of the longer M–P or M–As bonds the M···M separations in **1–3** are considerably greater than those in **5** and **6** and are comparable to the value observed in **7**. In addition the M_2E_2 cores are slightly folded whereas the M_2N_2 cores are rigorously planar. A similar folding was observed for the structure of the bis{μ-bis(trifluoromethyl)phosphido}hexacarbonyldiiron species, $Fe_2(CO)_6\{\mu\text{-}P(CF_3)_2\}_2$.[36] Another feature of interest of the structural data in Table II concerns the M–N terminal bond lengths. The distances seen in the homoleptic amides **5** and **6** are somewhat longer than those in complexes **1–3**. This may be a consequence of the greater crowding in **5** and **6** as a result of the shortness of the bridging M–N bonds in comparison to their phosphorus or arsenic analogues. The greater crowding in **5** and **6** is also manifested in their tendency to dissociate into monomers in solution[28] and the gas phase[23] whereas **1–3** do not readily display this tendency. The bridging Mn–P, Fe–P, or Mn–As distances in **1** to **3** are indicative of fairly strong bonding. For example, in the case of **5** and **6**, the Mn–N (bridging) and the Fe–N(bridging) distances are 2.174 (3) and 2.086 (3) Å. If the nitrogen radius 0.7 Å is subtracted and the phosphorus radius (1.11 Å) is added to these values, the predicted Mn–P and Fe–P bond lengths are 2.584 and 2.496 Å. These predicted lengths are significantly longer than those found in Table II.

Electronic Absorption Spectra. Solutions of compounds **1–3** in hexane all show significant absorptions in the UV/vis region as summarized in Table III. This is in sharp contrast to the spectra of the manganese(II) and iron(II) amide starting materials **5** and **6**, which have essentially featureless spectra with very weak absorptions. This is presumably due to the weak nature of the d–d transitions for the high-spin d^5 and d^6 configurations. Compounds **1–3**, however, have well-defined spectra. For example, a hexane solution of the black-red crystals of compound **2** has a fairly strong absorption (ϵ = 1630) at 20 000 cm^{-1} and a weaker absorption (ϵ = 171) at 12 500 cm^{-1}. The spectra of compounds **1** and **3** are similar, and both of them possess two absorptions. The more intense spectra observed in **1–3** are presumably due to replacement of an amide bridge with the heavier phosphide and arsenide homologues. It is also notable that the intensities of the absorptions for the arsenic derivative **3** are greater than those of the phosphorus species **1**. These data point to a ligand-to-metal charge-transfer mechanism as the origin of the absorptions. In this process, electron density is transferred from an orbital of mostly ligand character to a metal orbital. The orbitals that are involved in this process in complexes **1–3** are not known with certainty. Nonetheless, the relatively weak nature of the M–P or M–As σ bonds suggest that the σ levels may be high enough in energy to enable

(28) Bradley, D. C.; Fisher, K. J. *J. Am. Chem. Soc.* **1971**, *93*, 2050.
(29) Power, P. P. *Comments Inorg. Chem.* **1989**, *8*, 177.
(30) Issleib, K. *Z. Chem.* **1962**, *2*, 163. Issleib, K., Fröhlich, H. O. *Chem. Ber.* **1962**, *95*, 375. Issleib, K., Wenschuh, E. *Z. Naturforsch.* **1964**, *B19*, 199.
(31) Pestana, D. C.; Power, P. P. *J. Am. Chem. Soc.* **1989**, *111*, 6887; *Inorg. Chem.* **1991**, *30*, 528.
(32) Baxter, S. G.; Cowley, A. H.; Davis, R. E.; Riley, P. E. *J. Am. Chem. Soc.* **1981**, *103*, 1699.
(33) Ni, C.; Zhang, Z.; Xie, Z.; Qian, C.; Huang, Y. *Jiegou Huaxue* **1986**, *5*(3), 181.
(34) Arif, A. M.; Jones, R. A.; Kidd, K. B. *J. Chem. Soc., Chem. Commun.* **1986**, 1440.
(35) Rheingold, A. *Chem. Rev.* **1990**, *90*, 169.
(36) Clegg, W. *Inorg. Chem.* **1976**, *15*, 1609.

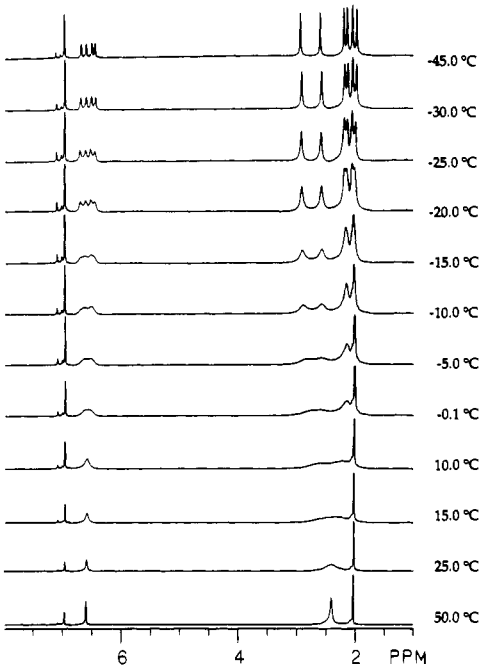

Figure 5. Stacked plot of the variable-temperature ^1H NMR spectra of **4** in C_7D_8.

an electronic transition from a σ orbital to one of the metal d orbitals to be observed in the visible region.

Magnetism and NMR Studies. The magnetic moments of compounds **1–3** were determined by the Evans method.[18] These values are also presented in Table III. They are consistent with a high-spin configuration for Mn and Fe species. The values obtained are similar to those seen for **5** and **6**.[23] A high-spin configuration is expected in view of the three-coordinate, C_{2v} geometry of the metals that gives rise to a relatively weak ligand field. The values for the magnetic moments are, with the exception of that for compound **1**, greater than the spin-only values, indicating that there is a significant orbital contribution to the magnetic moment.

The ^1H NMR spectra of **1–3** all display isotropically shifted peaks as a result of the presence of unpaired electrons. This is notable because ^1H NMR spectra of Mn(II) compounds are often difficult to observe owing to slow electron exchange that causes rapid relaxation. Complete assignments are not possible for all compounds without extensive isotropic labeling and/or substitution studies. However, a comparison of ^1H NMR spectrum of **2** with that of $Fe[N(SiMe_3)_2]_2$ (**6**),[37] at room temperature, suggests that the three peaks at 12.11, 0.11, and −6.58 ppm may be assigned to the dimesitylphosphido groups whereas the remaining broad peak at ~53 ppm is very close to one of the peaks seen in the spectrum of $Fe[N(SiMe_3)_2]_2$ and so is in all probability due to the $-N(SiMe_3)_2$ terminal resonance.

The ^1H NMR spectrum of **1** at room temperature displays a complicated pattern with seven different peaks observed in the range −160 to +170 ppm. If the sample is heated to 85 °C, this pattern becomes much simpler, and only four peaks are observed at this temperature. This simpler pattern resembles, in some respects the spectrum of **2**. The peak at 76 ppm may be tentatively assigned of the to the terminal $-N(SiMe_3)_2$ groups. The remaining broad peak at 25 ppm is probably due to the meta hydrogens of the mesityl groups. Two narrower peaks at 5.0 and −0.1 ppm are probably due to the *o*- and *p*-methyl groups.

Variable-temperature ^1H NMR spectra of **4** are displayed as a stacked plot in Figure 5. It has similar characteristics to the plot for Mes_2PPMes_2.[32] At −45.0 °C, 10 peaks were resolved and these are due to four different meta hydrogens, four different *o*-CH_3 groups, and two different *p*-Me groups. Four downfield methyl peaks at 2.9, 2.56, 2.17, and 2.11 ppm and two upfield methyl peaks at 2.03 and 1.96 ppm could be assigned to four *o*-CH_3 groups and two *p*-CH_3 groups, respectively. When the solution is heated to 50 °C, the peaks broaden and coalesce until only three peaks remain. These peaks are now due to equivalent meta H, *o*-CH_3 and *p*-CH_3 groups. This behavior matches that of the phosphorus analogue very closely.[32] For **4**, the coalescence temperature for the dynamic process was 273 K for the meta peaks. Substitution of the appropriate parameters and $\Delta\nu = 101$ Hz into the relevant equation[38] reveals that the barrier to this dynamic process is about 13.0 kcal/mol.

In summary, three heteroleptic amidomanganese(II) and amidoiron(II) phosphide and arsinide and tetramesityldiarsane compounds have been characterized. Attempts to obtain the corresponding homoleptic diphosphido or diarsenido derivatives by the same methods have not been successful owing to the formation of the diphosphane or diarsane. The presence of one hetero group in addition to the phosphide or arsenide appears to be necessary, at least in these systems, to enable the isolation of stable complexes.

Acknowledgment. We than the donors of the Petroleum Research Fund, administered by the American Chemical Society, for financial support of this work and Steven C. Shoner and Karin Ruhlandt-Senge for experimental assistance and useful discussions.

Supplementary Material Available: A table containing full details of the X-ray data collection and refinement and full tables of atom coordinates, bond distances and angles, hydrogen atom coordinates, and anisotropic thermal parameters (29 pages); tables of structure factors (129 pages). Ordering information is given on any current masthead page.

(37) Chen, H.; Power, P. P.; Shoner, S. C. Unpublished work. See also: Chen, H.; Bartlett, R. A.; Dias, Rasika H. V.; Olmstead, M. M.; Power, P. P. *J. Am. Chem. Soc.* **1989**, *111*, 4338.

(38) Kost, D.; Carlson, E. H.; Raban, M. *J. Chem. Soc., Chem. Commun.* **1971**, 656.